El Niño–Southern Oscillation–based index insurance for floods: Statistical risk analyses and application to Peru

Abedalrazq F. Khalil,[1] Hyun-Han Kwon,[1] Upmanu Lall,[1] Mario J. Miranda,[2] and Jerry Skees[3]

Received 23 June 2006; revised 18 June 2007; accepted 3 July 2007; published 17 October 2007.

[1] Index insurance has recently been advocated as a useful risk transfer tool for disaster management situations where rapid fiscal relief is desirable and where estimating insured losses may be difficult, time consuming, or subject to manipulation and falsification. For climate-related hazards, a rainfall or temperature index may be proposed. However, rainfall may be highly spatially variable relative to the gauge network, and in many locations, data are inadequate to develop an index because of short time series and the spatial dispersion of stations. In such cases, it may be helpful to consider a climate proxy index as a regional rainfall index. This is particularly useful if a long record is available for the climate index through an independent source and it is well correlated with the regional rainfall hazard. Here El Niño–Southern Oscillation (ENSO) related climate indices are explored for use as a proxy to extreme rainfall in one of the districts of Peru, Piura. The ENSO index insurance product may be purchased by banks or microfinance institutions to aid agricultural damage relief in Peru. Crop losses in the region are highly correlated with floods but are difficult to assess directly. Beyond agriculture, many other sectors suffer as well. Basic infrastructure is destroyed during the most severe events. This disrupts trade for many microenterprises. The reliability and quality of the local rainfall data are variable. Averaging the financial risk across the region is desirable. Some issues with the implementation of the proxy ENSO index are identified and discussed. Specifically, we explore (1) the reliability of the index at different levels of probability of exceedance of maximum seasonal rainfall, (2) the effect of sampling uncertainties and the strength of the proxy's association to local outcome, (3) the potential for clustering of payoffs, (4) the potential that the index could be predicted with some lead time prior to the flood season, and (5) evidence for climate change or nonstationarity in the flood exceedance probability from the long ENSO record.

Citation: Khalil, A. F., H.-H. Kwon, U. Lall, M. J. Miranda, and J. Skees (2007), El Niño–Southern Oscillation–based index insurance for floods: Statistical risk analyses and application to Peru, *Water Resour. Res.*, *43*, W10416, doi:10.1029/2006WR005281.

1. Introduction

[2] It is well recognized [*Martin et al.*, 2001; *Podesta et al.*, 2002; *Rosenzweig et al.*, 2002; *Stigter et al.*, 2005; *Wall and Smit*, 2005] that climate hazards contribute significantly to agricultural losses and hence to the vulnerability of the rural poor, especially in developing countries. Public sector investments in crop insurance in many countries have often been problematic. Often the insurance has been tied to the insured farm's yield, with heavily subsidized premiums. This has led to inefficient responses, such as growing crops in high climate risk areas, asymmetry of information (e.g., farmers know more about their risk than the insurer), manipulation (e.g., farmer skews management practice to negatively impact crop yield), high administrative costs associated with loss verification and program administration, a slow payout of benefits, and large payouts in catastrophic years that are difficult to reinsure. Further, it is very difficult to analyze the potential losses and payouts and for extreme climate events (e.g., one in a 50 or 100 year event) there is little data available to support rare events analysis. Finally, the risk exposure in such cases is typically correlated across the group insured, rendering it difficult to insure. Consequently, index insurance schemes are being advocated and implemented in the public and private sectors [*Changnon et al.*, 2001; *Duncan and Myers*, 2000; *Hess et al.*, 2005; *Skees et al.*, 1997; *Skees and Barnett*, 1999; *Skees and Reed*, 1986]. In the present paper, we consider a country-scale index (re)insurance product, rather than a product aimed at individual farmers.

[3] Index insurance seeks to address several of the problems noted above by tying the payoff to a trigger event determined by an index threshold that is quantifiable, unambiguous, and is ideally specified and measured by a credible third party independent of the insurer and the insured. The index insurance formulated here is immune

[1]Department of Earth and Environmental Engineering, Columbia University, New York, New York, USA.
[2]Department of Agricultural, Environmental, and Development Economics, Ohio State University, Columbus, Ohio, USA.
[3]Department of Agricultural Economics, University of Kentucky, Lexington, Kentucky, USA.

0043-1397/07/2006WR005281$09.00

against adverse selection since the index is based on widely available information where little information asymmetries could be exploited. Similarly, the moral hazard is minimized because the indemnity does not depend on the individual crop production or farmer effort. Typically, if an event determined by the index is triggered, the contract provides a payoff that is related to the risk assessed for the triggering event. Those with insurable risk could buy such contracts, and the effective premium per value insured is the same for all buyers. The index insurance product could be purchased by a microfinance authority or local state or district authority to facilitate rapid loans and relief in the event of a disaster that matches the triggered event, or be purchased directly by individual farmers. Ideally, the economics of an insurance product should be closely related to the anticipated losses. In the case of index insurance, this could be accomplished by each buyer having knowledge of the risk associated with the trigger, the unit contract price, the payoff stream, the buyer's budget and an assessment of potential losses. Subsidies could be provided to the poorer segments, if needed, through loans or grants for purchasing index insurance contracts. The Commodity Risk Management Group of the World Bank is actively researching and implementing weather index insurance strategies in a number of countries with help from major reinsurance companies and the International Research Institute for Climate and Society at Columbia University.

[4] A weather-based index could be based on rainfall or temperature recorded at a specific place, and the payoff could be a lump sum or be proportional to the deviation of the index from the trigger event [*Bardsley et al.*, 1984; *Luo et al.*, 1994]. The rainfall-based index could be used to develop products for drought or flood, and could include duration, severity and timing information in the index. A problem with developing a rainfall index is that rainfall can vary dramatically in space, and the chosen rain gauge may not be representative of the location insured. Further, rain gauge records in developing countries can be sparse and short, making it difficult to assess the probabilities of extreme events. The actuarial analysis associated with a rainfall index is further confounded by the possibility that anthropogenic climate change may lead to changing extreme event risk over time.

[5] Area-based indices that are related to the decline of areally averaged yields over a region have also been proposed [*Miranda*, 1991; *Miranda and Glauber*, 1997]. These address the issue of manipulation by an individual farmer, but still require time and information to compute the actual yields and hence will have slower payoffs and higher administrative costs compared to a rainfall index.

[6] *Skees et al.* [2005, p. 19] discuss "basis risk" associated with weather index insurance products. They note that a "major challenge in designing an index insurance product is minimizing basis risk." In the current context, basis risk "occurs when an insured has a loss and does not receive an insurance payment sufficient to cover the loss (minus any deductible). It also occurs when an insured has a loss and receives a payment that exceeds the amount of loss." The effectiveness of index insurance as a risk management tool depends on how positively correlated farm yield or revenue losses are with the underlying index. The basis risk inherent in index insurance products has been widely discussed in the scholarly literature. Much less discussed is that basis risk also exists with farm-level, multiple-peril, and crop yield insurance. Typically, simple statistics about the error of small sample estimates used to calculate the central tendency in farm-level yields, it can be easily demonstrated that these procedures sometimes generate large mistakes when estimating expected farm-level yield. Thus basis risk occurs not only in index insurance but also in farm-level yield insurance [*Skees et al.*, 2005].

[7] For the purposes of the current paper, given that we are focused on the country of Peru or some aggregator as the recipient of the insurance product, the discussion above maps into a need to examine the magnitude of the risk that may be induced at the regional level by using the proposed El Niño–Southern Oscillation (ENSO) index relative to the risk that may be induced by a finite sample size associated with a regional rainfall index used as a trigger for payoffs. This aspect of risk is examined in section 3.1 to (1) see how one could establish whether the external proxy leads to substantially higher basis risk than the regional proxy, and (2) assess this for the current data set.

[8] An example of a proposal to use ENSO index insurance is the case for hurricane incidence and the resulting damages for South eastern US. Here, a customized pricing policy that provides an appropriate hedge to insurers and conventional contracts to the insured was devised in the context of trading securities conditioned on the ENSO state [*Chichilnisky and Heal*, 1998]. The connection between hurricane incidence or damage and the ENSO indices is not explored in this paper. Other similar proposals have been made, but to date no systematic statistical evaluation of how an ENSO index's behavior relates to a local proxy has been made in the context of index insurance and risk transfer. This paper partly attempts to fill in this knowledge gap.

[9] The effect of the Southern Oscillation on precipitation has been examined in numerous studies [*Ropelewski and Halpert*, 1989, 1987; *Woolhiser et al.*, 1993; *Tapley and Waylen*, 1990]. Here, we explore the identification and use of an index that would use ENSO-related data from NOAA for flooding in the Northern regions in Peru. If such an index could be effective for risk transfer, it would have some advantages over either weather index or area-based yield indices, since it is rapidly available, cannot be manipulated by those who are insured, and may relate to the physical mechanisms that govern regional precipitation and flooding. Rainfall and streamflow records for Peru are sparse, short and intermittent, as may be expected in a developing country. There is some concern on the part of external reinsurers that since the rainfall data are collected by local government agencies, they could be manipulated for payoffs if local agencies were purchasing the insurance. Hence the use of an externally measured and provided index is desirable. Over 150 years of data are available for a suite of ENSO indices from NOAA and other sources.

[10] Experts from the Peruvian agriculture ministry (MINAG), weather service (SENAMHI), and natural resources (INRENA) agencies generally agree that floods associated with major El Niño climatic events have been responsible for the greatest damage to agriculture in Piura over the past 50 years. The work presented here was motivated by a request to develop an index insurance product that could be used for agricultural insurance by

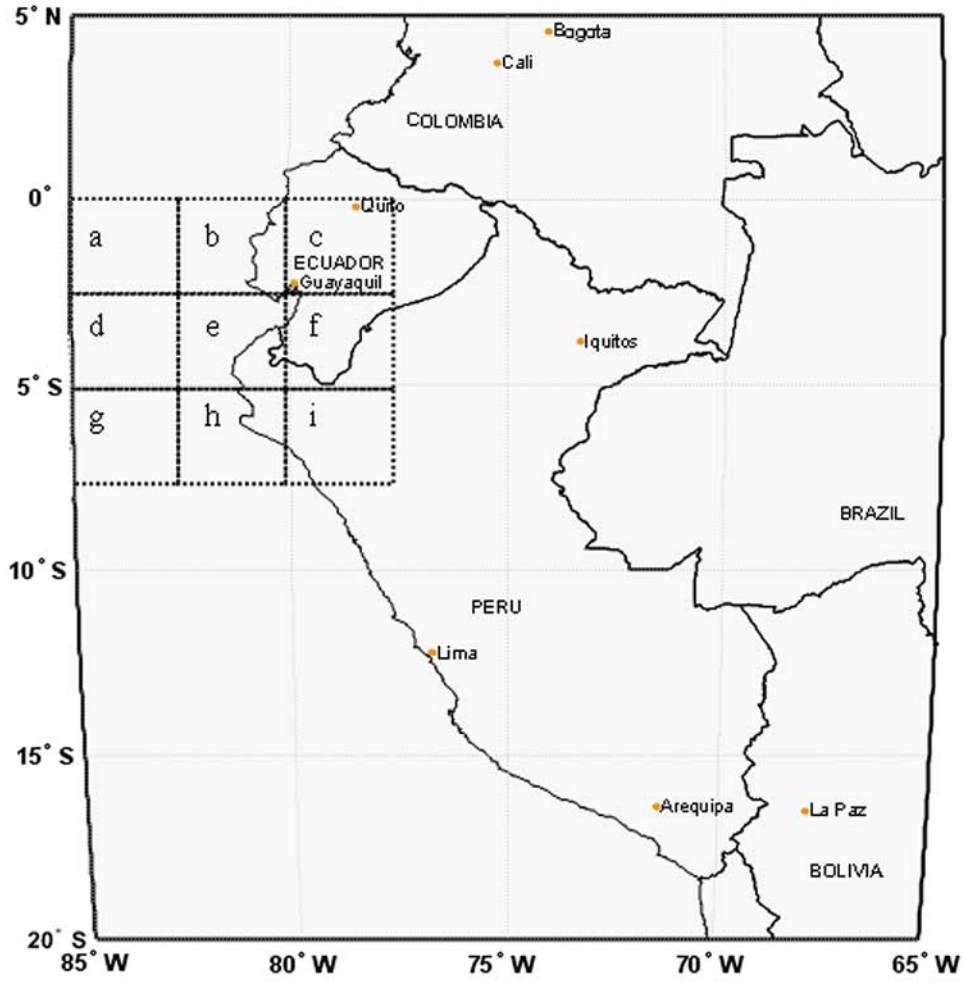

Figure 1. NOAA/CPC CMAP rainfall data grid elements used in the study. The Piura region overlaps with grid box e. This is the CMAP grid box used in our study.

regional governments or microfinance institutions in Peru. To finance large losses associated with extreme catastrophic flooding that accompany the warming of the Pacific Ocean (El Niño conditions), it is advisable to consider an external private sector insurer/reinsurer. Extreme flooding creates many problems in the Northern regions of Peru. However, agriculture is the primary target for this ENSO insurance product. The 150 years of data for several ENSO indices were considered for the development of an ENSO insurance for Peru. The specific questions of interest were:

[11] 1. Does one of the ENSO-related indices routinely available from NOAA correspond to flood occurrence in the region of interest in Peru?

[12] 2. Can one identify an insurance payoff trigger level using the "best" ENSO index for Peru that corresponds to the regional rainfall/flood exceedance probability at a desired level? What is the statistical relationship between the ENSO index and the regional rainfall based on the short records available? Can multiple trigger levels of the ENSO index be determined to correspond to multiple flood exceedance probabilities, and shown to be consistent and effective in predicting average annual flood risk for these extreme events? What is the risk due to sampling uncertainty associated with the use of the index, as related to (1) the regression sample size, and (2) the insurance contract duration?

[13] 3. What is the potential for clustered (serially correlated) payouts if the ENSO-based triggers are used to define an index insurance policy?

[14] 4. Is the average payout frequency corresponding to a particular ENSO trigger as inferred from the 150+ year record of the index unbiased?

[15] 5. Is it consistent with the frequency estimated in developing the index from the shorter ENSO index and rainfall data? Does using the 150 year ENSO proxy translate into a lower or higher risk due to sampling uncertainty as compared to using a regional rainfall index based on 50 years of data? Are there any trends in the exceedance frequency of the trigger index insurance level that are evident from the longer record suggesting that there may be nonstationarities related to anthropogenic climate change that need to be addressed in writing insurance policies covering the next 10 years?

[16] 6. With what lead time is the ENSO index, and specifically the trigger event predictable prior to the flood season; that is, how soon before the flood season should sales of the index insurance product be closed or premium/payoff adjusted?

[17] These questions are explored in a statistical analysis framework using readily available data on rainfall and ENSO climate indices. The data sets used and preliminary analyses are described in section 2. A logistic regression-

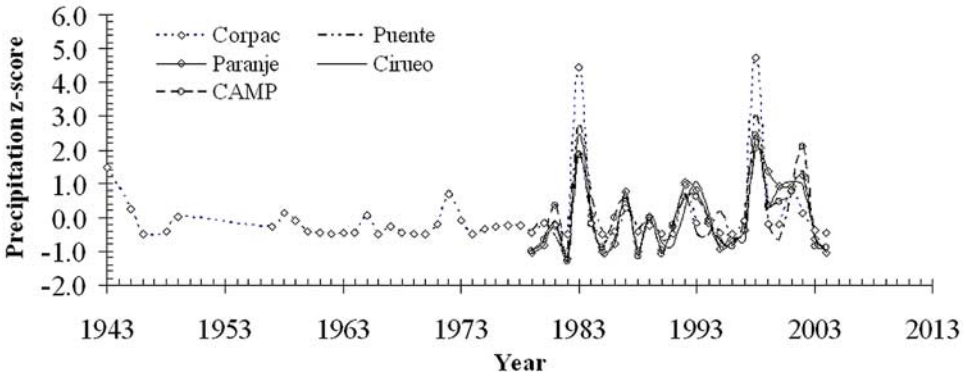

Figure 2. Normalized monthly maximum of January through April (JFMA) rainfall for the five rainfall series. Note the high correlation in these series and the variable length of record for the rain gauge data.

based investigation of questions two through five listed above is presented in section 3. A limited discussion of how an ENSO-based index insurance product could be applied to Peru and other settings concludes the presentation. Economic aspects of index insurance design and implementation are not discussed in this paper. The structural issues identified above as prerequisites to the potential introduction of ENSO index–based insurance are the focus of the paper.

2. Data and Preliminary Analysis

2.1. Developing a Proxy for Regional Floods

[18] Rainfall gauge data compiled by the Peruvian national weather service (SENAMHI) was available at seven locations in the Piura region. Total monthly rainfall, measured in millimeters, was available for these stations from 1943 to 2004. However, all seven series contained missing data to varying degrees over this period. The four rain gauges in the Piura Valley with the most complete records were CORPAC Piura, Puente Internacional, Parange Grande, and El Ciruelo. These were retained for consideration.

[19] The U.S. National Oceanographic and Atmospheric Administration's Climate Prediction Center (NOAA/CPC), provides a global rainfall data product called the Merged Analysis of Precipitation (CMAP), over 2.5° geographic arc grid elements using a blend of rain gauge data and satellite data. The satellite data are derived from five different sources: GPI, OPI, SSM/I scattering, SSM/I emission and MSU. These satellite data are blended with the NCEP/NCAR reanalysis model output of the global coverage monthly precipitation values. The resulting data set [*Xie and Arkin*, 1996, 1997; *Xie et al.*, 1996] is available as a series of monthly values from 1979 to 2004. The CMAP data possesses some desirable qualities for the construction of a proxy for flood-related losses for the Piura region. Since the data in this series are spatially averaged, they are likely to provide a better measure of flood conditions over the entire Piura catchment than rain gauge measurements taken at scattered points. Monthly rainfall data estimates from this source from 1979 to 2004 were secured for the nine grid elements shown in Figure 1. Of these, grid box (e) was selected as representative of the regional rainfall. The correlation of the monthly rainfall in this grid box with the monthly rainfall from each of the 4 rain gauges considered is greater than 0.75 for the common period of record.

[20] The regional rainfall proxy for flood-related losses is now constructed as follows: First, for each of the five (CMAP and 4 rain gauges) rainfall data series, the maximum monthly rainfall recorded during the principal growing season of January through April was determined for each year. Second, for each of the five series, the maximum January–April rainfall for each year was normalized to a z score by subtracting the sample mean and dividing by the sample standard deviation of the series (see Figure 2). Third, the maximum z score across all five series was taken each year as a measure of the annual flood potential throughout the Piura region. The data set formed covered the period from 1943 to 2004 and has values for 53 of these years. Note that all the rainfall series (CMAP and gauge) show high rainfall in 1983, 1993, 1998 and 2002 which are El Niño years. However, note that some series indicate a high rainfall event in 1992 while others have a high rainfall event in 1993.

2.2. Identifying a Suitable ENSO Index

[21] Recall that the available regional rainfall/flood proxies are relatively short, and that regional floods are believed to be strongly influenced by the El Niño–Southern Oscillation (ENSO). A variety of ENSO indices synthesized from observed and reconstructed Sea Surface Temperature (SST) are available at a monthly resolution dating back to 1856. The longer record provides an opportunity to test the reliability, predictability and stationarity of a proposed index for agricultural flood insurance in Peru. Further, we are interested in using a time series for index insurance whose data are (1) collected by an external third party, (2) reported rapidly through a public channel, and (3) relevant for floods in Piura, Peru. In this section we do a preliminary evaluation and selection of one of the readily available SST time series that is regularly updated on NOAA websites (http://www.cdc.noaa.gov/cdc/data.cmap.html).

[22] A linear correlation map of the regional flood proxy defined by the z scores of the maximum monthly rainfall in the growing season with the 1943–2004 January–April maximum of Pacific Sea Surface Temperature data in the general ENSO region is presented in Figure 3. The highest correlations (>0.8) between sea surface temperature and the regional flood proxy series are associated with the equatorial region just off the Peruvian coast. This is also the region typically identified with El Niño events. ENSO indices that represent gridded averages of SSTs in the equatorial Pacific

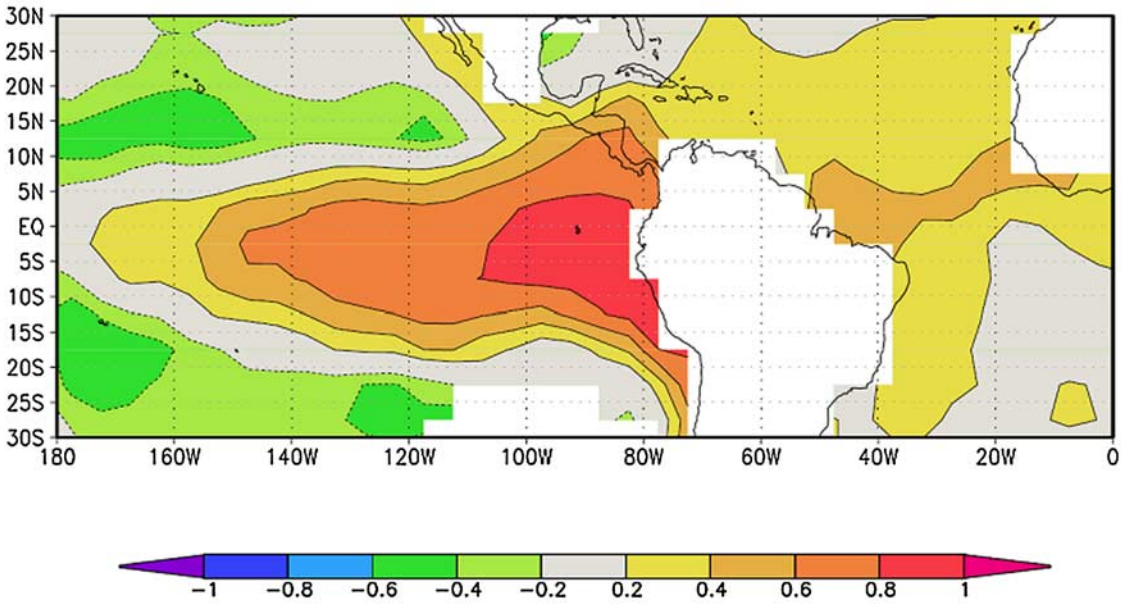

Figure 3. Correlation between sea surface temperature and the regional flood proxy series for Piura, using 53 years of data from 1943 to 2004. Correlations above 0.27 in absolute value are statistically different from 0 at a 5% significance level.

Ocean are routinely distributed by NOAA. These include the NINO1, NINO2, NINO3, and NINO4 indices identified in Figure 4 and the NINO1.2 and NINO3.4 indices which are composites of NINO1 and 2, and NINO3 and 4 respectively. The January–April seasonal maxima of these 6 indices were considered as candidates for correlating to the regional flood proxy over the concurrent period of record (1943 to 2004).

[23] The initial correlation analysis suggested that the NINO1.2 index was likely to be the best candidate as a surrogate for the regional flood proxy. A scatterplot of the regional flood proxy and the January–April NINO1.2 index is shown in Figure 5. We note that while the correlation between the regional flood proxy and the NINO1.2 series is high, the explanatory strength of NINO1.2 is weak except for the larger rainfall (flood) events which correspond to the large NINO1.2 values observed. Thus flood magnitudes and losses above some threshold may be proportional to NINO1.2 exceedances above a corresponding threshold, and NINO1.2 may be a useful proxy index for extreme regional floods for which insurance is desired. The concern with respect to the stationarity of NINO1.2 time series was tested using the Mann-Kendall method [*Salas*, 1992] for trend detection and the null hypothesis of no trend was not rejected at 5% significance level. In addition, a trend test was performed for the coral-derived record of NINO3 index [*Mann et al.*, 1998a, 1998b; *Mann and Park*, 1994] that covers 1650–2004 and the null hypothesis of no trend was not rejected at 5% significance level.

3. Identifying a Trigger Value of the NINO1.2 Index for Piura Flood Index Insurance

[24] If the regional flood proxy series were used directly to specify a trigger threshold for index insurance, then one could specify the trigger level as the value of the series corresponding to a desired probability of exceedance, p_{exc}, e.g., 0.1, corresponding to an event with a return period of 10 years. The corresponding threshold could be estimated from an empirical or fitted cumulative distribution function for the 1943 to 2004 record of the series, under the assumption that the maximum monthly rainfall in each

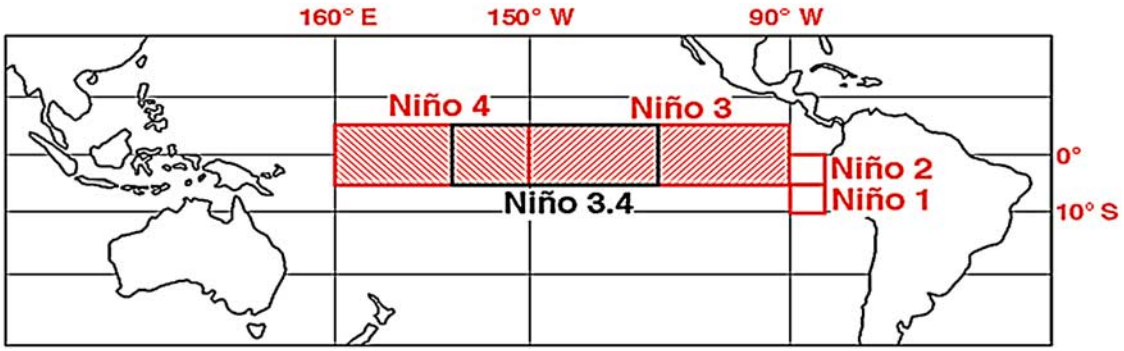

Figure 4. Regions of Pacific Ocean for which ENSO indices are compiled [*Glantz*, 2001].

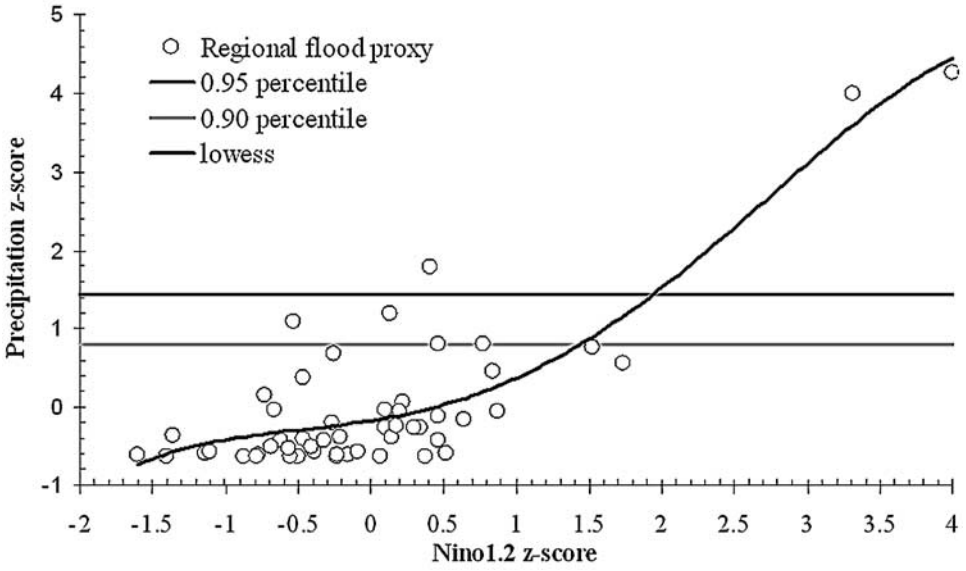

Figure 5. Regional flood proxy series for Piura versus January–April maximum of NINO1.2 index using 53 years of data between 1943 and 2004. The correlation between the two series is 0.79 (Spearman), 0.94 (rank). The two horizontal lines represent the 90th and 95th percentiles of the distribution of the regional flood proxy based on 53 years of data, and the solid curve represents a lowess smooth [*Cleveland*, 1979] of the data with a span of two thirds of the data.

January–April season is independent and identically distributed. However, as indicated earlier, this is a relatively short record for such estimates, and moreover we are interested in using the NINO1.2 series as the index for Peru. Consequently, we use a multistep strategy to define an appropriate trigger level using the NINO1.2 series, and to then test the performance of the trigger. This strategy is sketched out below and then its application to the data is described.

[25] 1. Let us say that p_{exc} is 0.1. Then we can identify (from the cumulative distribution function of y), a corresponding threshold y*, such that the regional flood proxy is exceeded on average with probability p_{exc}, i.e., E[p(y > y*)] = 0.1, the 90th percentile of the regional flood proxy index.

[26] 2. We seek a trigger value x* for NINO1.2, such that on average the probability of exceedance of the corresponding threshold for the regional flood proxy series, is the desired probability p_{exc}. Given a rank correlation between y and x of 0.94, their mutual relationship is monotonically increasing, and hence we expect that if a certain threshold x* is exceeded, then on average a corresponding threshold y* is exceeded with some probability. The strategy is to try to identify such an x*, and then test its performance.

[27] 3. Given the assumption that y is an independent and identically distributed random variable, it is reasonable to consider the binomial process, v, (v = 1 if y > y*, 0 else). Now, if we consider a logistic regression of v on x, the NINO1.2 index, we can estimate the conditional probability E[p(v|x)]. If E[p(v|x)] is greater than or equal to 0.5, then we expect an insurance payout; that is, on average we expect an exceedance of the threshold y* corresponding to p_{exc}. Restated, the appropriate trigger level, x* for NINO1.2 could be identified as the NINO1.2 value such that the average conditional probability estimated from the logistic regression is 0.5.

[28] This process is now applied to the 1979 to 2004 data for the Peru regional flood proxy series, y_t, and the NINO1.2 time series, x_t. We consider two candidate levels for the exceedance probability, 0.1 and 0.05, corresponding to the events with return periods of 1 in 10 and 1 in 20 years. From the empirical cumulative distribution function of y, we identify the corresponding thresholds, y*, as 0.81 and 1.43, respectively (see Figure 5). These thresholds are then used to construct the binary series v_{1t}, and v_{2t}, that represent exceedances of the 1 in 10 and 1 in 20 year thresholds respectively.

[29] The corresponding logistic regression models for the two thresholds are then

$$v_1: \quad \log\left(\frac{p_1}{1-p_1}\right) = a_1 + b_1 x$$
$$v_2: \quad \log\left(\frac{p_2}{1-p_2}\right) = a_2 + b_2 x \tag{1}$$

[30] Given the monotonicity assumption with respect to the relationship between y and x, we further require that

$$a_1 + b_1 x > a_2 + b_2 x \tag{2}$$

[31] Once the model coefficients are evaluated the probability, p, that the regional flood proxy series will exceed the specified threshold, conditional on a NINO1.2 value, x, is estimated as

$$p = \frac{\exp(a + bx)}{1 + \exp(a + bx)} \tag{3}$$

Table 1. Selected Logistic Regression Results From Bayesian Estimation

Model	1 in 20 Years		1 in 10 Years	
	a	*b*	*a*	*b*
Posterior mean	2.75	−5.83	1.72	−2.29
Standard deviation	1.13	2.06	0.20	0.22
0.025 percentile	1.02	−10.7	1.5	−2.4
Median	2.52	−5.5	1.72	−2.27
0.975 percentile	5.44	−2.98	2.31	−1.66
Chi square	13.15	13.15	4.31	4.31
Regression *P* value	7.6E-05[a]	7.6E-05	0.018	0.018

[a]Read 7.6E-05 as 7.6×10^{-5}.

[32] The two logistic regression models are solved simultaneously in a Bayesian framework. Noninformative priors are assumed for each of the parameters a_i, and b_i, and their optimal values are selected through a maximization of the posterior likelihood associated with the logistic regression models while imposing the monotonicity constraint above. A Markov Chain Monte Carlo procedure is used. In particular, the Gibbs sampling approach to MCMC [*Gilks et al.*, 1995] has been used in this study. The Gibbs sampler was implemented using the BUGS software [*Spiegelhalter*, 1998; *Spiegelhalter et al.*, 2002]. The prior distributions were specified as the normal distribution (i.e., $a_i \sim N(0.0, 1000)$ and $b_i \sim N(0.0, 1000)$). We chose to run three chains simultaneously searching for optimal parameters. The evolution of each chain was monitored to check for convergence to a common value. This approach to use constrained Bayesian estimation for the parameters of multiple logistic regressions while enforcing a monotonicity constraint is novel to our knowledge, and could be used for other conditional distribution function estimation problems.

[33] The results are summarized in Table 1, and illustrated in Figure 6. Fitting both models simultaneously constrains their results to be consistent with the monotonic response (no crossing of the two curves) desired (Figure 6). The trigger levels x* of NINO1.2 are identified for each p_{exc} in Figure 6 as the values that correspond to the E[p(v|x] = 0.5. The payout events (identified as $v_t = 1$ or 0) corresponding to the NINO1.2 triggers identified x are illustrated in Figure 7 for each of the two p_{exc} levels.

3.1. Risk Induced by Sampling Variability

[34] The temporal risk associated the regional rainfall index could be derived analytically; however, a bootstrapping procedure is employed for a consistent comparison between ENSO trigger and Logistic Model for rainfall exceedance. The temporal risk associated with the regional rainfall index as a function of the sample size *n*, used for estimating the trigger at the qth percentile, and the sample size *m* used as the length of the insurance contract over which payout performance is assessed.

[35] First, the temporal risk associated with the regional rainfall index as a function of the sample size *n*, used for estimating the qth percentile used as a trigger, and the sample size *m* used as the length of the insurance contract over which payout performance is assessed. This analysis can be done analytically, but here we use a bootstrap procedure so that a consistent design for comparison with the ENSO trigger and Logistic Model for rainfall exceedance is provided. Let y_q^* denote the qth quantile of the rainfall index estimated from a sample of size *n* (53 for our data). Let us say that a *m* year future period is of interest for the analysis of payoff outcomes. Then in a given *m* year period one may experience *k* exceedances of y_q^*, or a relative exceedance frequency of k/m instead of $(1 - q)$. On average, over many samples of size *m*, these frequencies will be equal. However, the variation from one sample to another is a measure of the temporal risk associated purely with the length of the period of performance of a contract. This is assessed by drawing 1000 samples of size *m*, with replacement from the original sample of size *n*, and estimating k/m for each such sample. The results for our data are illustrated in Figures 8 and 9 for $m = 10$ and 50, and for $q = 0.9$ and 0.95 respectively. As expected we note that the variability in realized exceedance frequency for the two triggers considered is higher for the shorter contract period.

[36] Second, we consider the variability in realized exceedance frequency if the ENSO index were used to

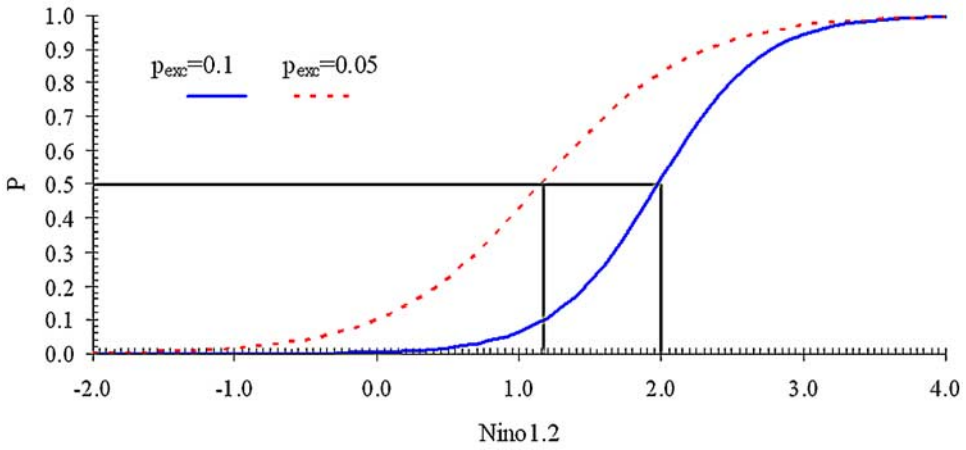

Figure 6. Predicted E[p|x] from logistic regression evaluated for the values of the NINO1.2 time series from 1856 to 2005, using the two models fit to the 1943–2004 data of NINO1.2 and the regional flood proxy series. The trigger levels are 1.17 and 2.05 for pexc = 0.1 and 0.05, respectively.

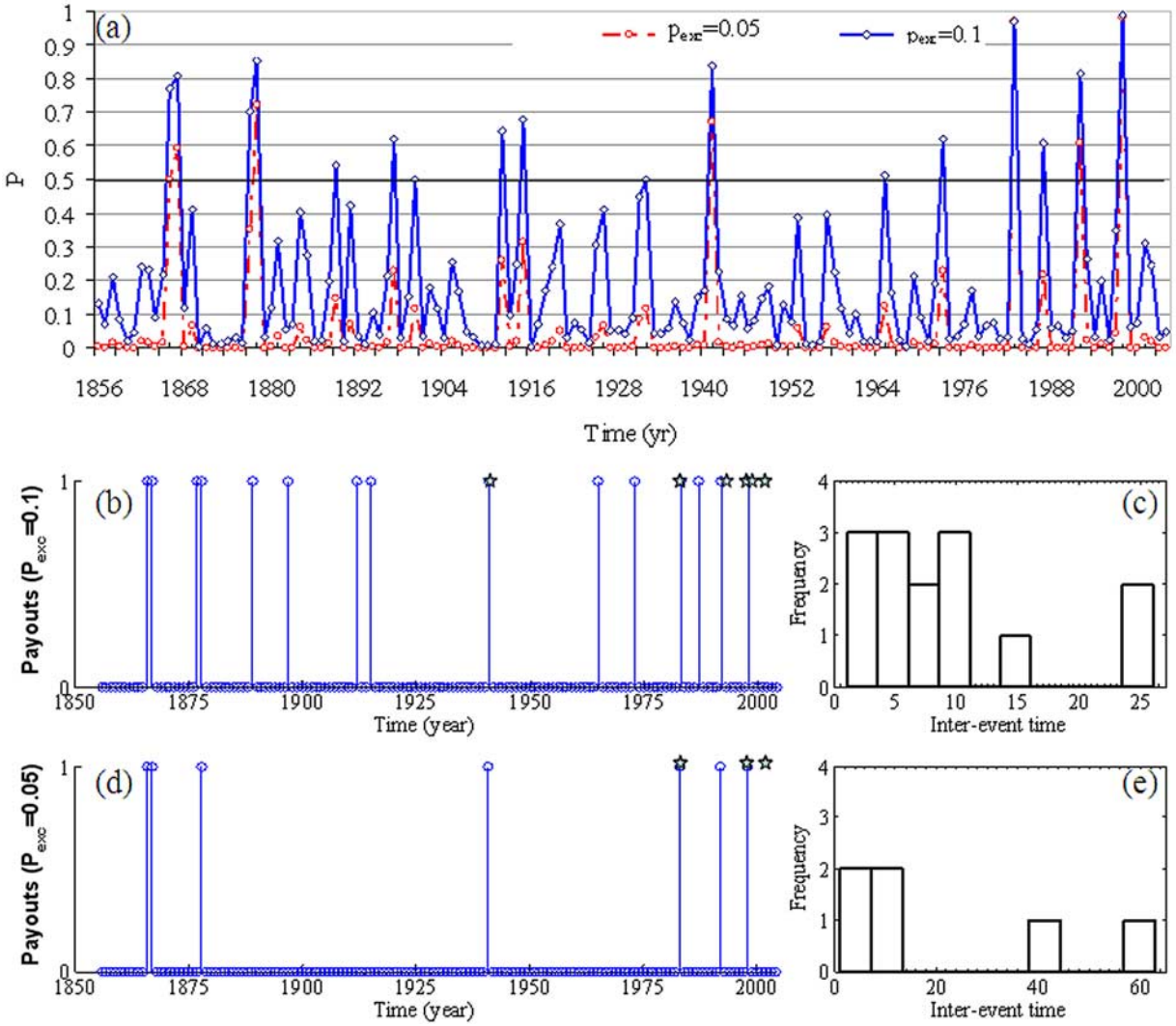

Figure 7. Time series of the E[p(v|x)] from the logistic regression and the payouts based on the NINO1.2 at two trigger levels corresponding to pexc = 0.1 and 0.05. The interevent time distribution corresponding to these thresholds is also illustrated. The payout years corresponding to the regional flood proxy series based on the 1943–2004 data are marked with stars, and those based on the NINO1.2 series are marked with circles.

predict rainfall exceedance using the Logistic Model. Two cases are considered. First we consider that the analysis is based purely on the sample size n (53) used for estimating the model parameters. Next, we consider that we actually have a much longer (150 years) proxy record available for the ENSO index and explore how this reduces the sampling uncertainty and hence the temporal risk. For this analysis, we have only considered a future contract operation period of m = 50 years.

[37] The posterior predictive distribution $f(p_j|x_j)$ for the probability of exceedance p_j of a rainfall threshold y_q^* given a new NINO1.2 observation x_j corresponding to the Logistic Model described in equations 1 to 3 is given as

$$f(p_j|x_j,\mathbf{x},\mathbf{v}) = \int f(p_j|\boldsymbol{\beta},x_j) f(\boldsymbol{\beta}|\mathbf{v},\mathbf{x}) d\boldsymbol{\beta} \tag{4}$$

where $\mathbf{x}$ is the original data sample of NINO1.2, $\mathbf{v}$ is the original binary sequence corresponding to the exceedance of y_q^*, and the $\boldsymbol{\beta}$ are the regression coefficients, and f(.|.) represents a conditional probability density function.

[38] Now if x_j is $\geq x^*$, the trigger that is established from the prior analysis, then the probability p_j^- that a payoff is declared and in reality a rainfall threshold exceedance does not take place is given as

$$p_j^- = \int_0^{0.5} f(p_j|x_j,\mathbf{x},\mathbf{v}) dp_j \tag{5}$$

[39] Similarly, if x_j is $<x^*$, then the probability p_j^+ that a payoff is not declared and in reality a rainfall threshold exceedance does take place is given as

$$p_j^+ = \int_{0.5}^{1} f(p_j|x_j,\mathbf{x},\mathbf{v}) dp_j \tag{6}$$

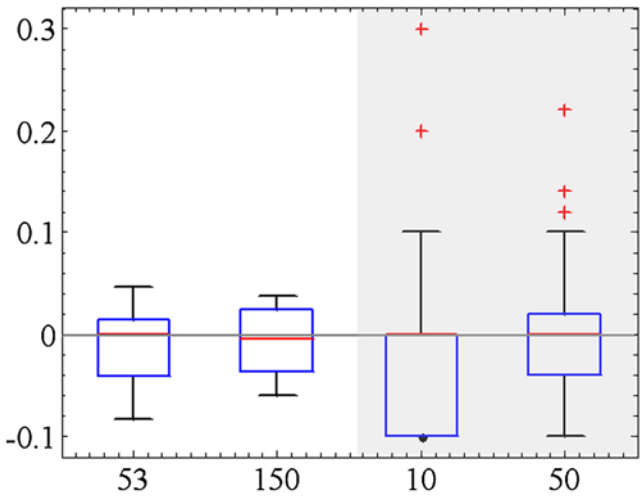

Figure 8. Basis risk at 0.1% trigger value applied on logistic regression for 53 years of NINO1.2 (unshaded) and for raw bootstrapping on the 53 years of precipitation data at different bootstrapping samples (shaded).

[40] Given these two statements, one can compute the variability in realized risk for a given future period of length m as

$$p^{+} = \sum_{j=1}^{m} p_j^{+}/m \quad \& \quad p^{-} = \sum_{j=1}^{m} p_j^{-}/m \tag{7}$$

[41] Now one can draw 1000 samples the NINO1.2 index of size m from the original data (53 years or 150 years) and estimate the statistics in equation 7 for each of these samples. The composition of these bootstrap samples then provides the predicted uncertainty distribution of payoffs corresponding to y_q^* given the original data used for regression and the sampling variability of the estimated logistic parameters, and the sampling variability of the NINO1.2 process. The resulting frequency distribution is illustrated also in Figures 8 and 9 for the both NINO1.2 proxy sample sizes and the two exceedance thresholds. We note that using the longer proxy series offers some reduction in the temporal risk, but in all cases the resulting temporal risk is comparable to that associated with the use of the rainfall index directly for the common comparison period of m = 50.

3.2. Time Series Attributes of Payouts Using the NINO1.2 Triggers

[42] In this section, we explore whether there are (1) trends in the payout frequency using the NINO1.2 index–based triggers, (2) the frequency distribution of the time between payout events, and (3) the potential for clustering or multiyear runs of payout events.

[43] The payout events (identified as v_t = 1 or 0) corresponding to the NINO1.2 triggers identified in Figure 6 for each of the two p_{exc} levels are illustrated in Figure 7. There are 15 payout events in 150 years corresponding to the p_{exc} = 0.1 trigger, and 7 payout events corresponding to p_{exc} = 0.05 trigger. Recall that the modeling process is based on the regional flood threshold that is exceeded with probability p_{exc}, using the short regional record, and that the NINO1.2 trigger is estimated from the logistic model using this threshold. A priori we hope but do not necessarily expect that the NINO1.2 trigger will be exceeded with the desired probabilities using the longer record. The correspondence between the event frequency realized in the 150 year NINO1.2 record, and that expected from the model fit for the shorter period using the p_{exc} of the regional flood proxy series is acceptable. Thus, at least on average, the NINO1.2-based index and trigger may reproduce the event frequencies for regional flood exceedance at the 0.1 and 0.05 levels, and is hence an unbiased basis for flood index insurance for Piura at these levels.

[44] The Mann-Kendall test for monotonic trend was applied to the two v_t series corresponding to each of the two p_{exc} levels. In each case, the null hypothesis of no monotonic trend was not rejected at a significance level of 5%. Thus, at least on this basis, nonstationarity (e.g., due to anthropogenic climate change) does not appear to be a significant problem in the existing record.

[45] The interevent frequency distribution of payout is also illustrated for each trigger level in Figure 10. The interevent distribution that is below 10 years data is characterized by high frequency in the historical data. Recall that the average interevent or recurrence time is expected to be 10 and 20 years respectively for the two thresholds. There seems to be some clustering of events at the p_{exc} = 0.1 threshold. This is explored further below.

[46] El Niño events are known to exhibit quasiperiodic behavior with a dominant period between 3 to 8 years. The likelihood that the NINO1.2 index will exceed a given threshold in runs of 2 or more consecutive years is consequently of interest to both the insurer and the insured. An assessment of the likelihood that the NINO1.2 index will exceed the p_{exc} thresholds of 0.05 and 0.1, in runs of 2 or more consecutive years was performed using spectral and raw bootstrap techniques. The raw bootstrap reshuffles all the data, and is used to provide an estimate of the probability distribution of run lengths under the assumption that the underlying climate signal has no memory. The spectral bootstrap preserves the autocorrelation function of the series

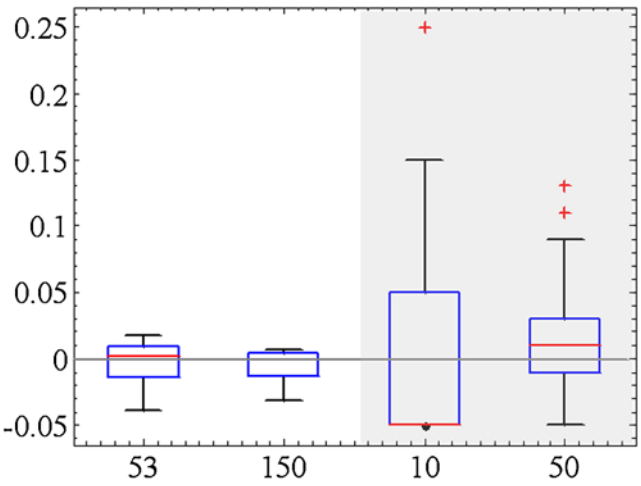

Figure 9. Basis risk at 0.05% trigger value applied on logistic regression for 53 years of NINO1.2 (unshaded) and for raw bootstrapping on the 53 years of precipitation data at different bootstrapping samples (shaded); *x* axis is in years.

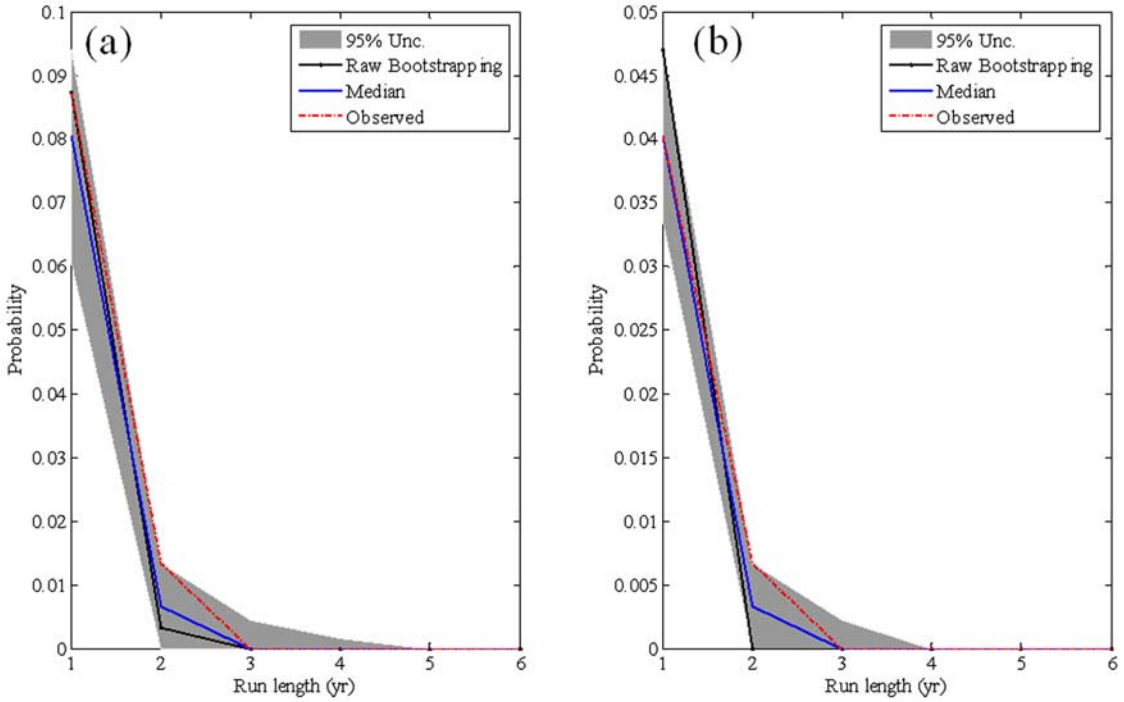

Figure 10. Run length per simulation as a result of logistic regression over 10,000 spectral and raw bootstrap samples, (a) pexc = 0.1 and (b) pexc = 0.05. The spectral bootstrap results include the median and the 2.5% and 97.5% percentiles across the 10,000 simulations. Only the median is provided for the raw bootstrap.

and allows us to estimate the likely probability distribution of different run lengths given that the series has memory.

[47] The spectral bootstrap technique fits an autoregressive model to the original time series of monthly NINO1.2 data and then simulates sequences from this model. Specifically, monthly NINO1.2 data were decomposed into their Fourier components

$$x_t = \sum_{j=1}^{N/2} A_j \sin(\omega_j t + \phi_j) \quad t = 1 \ldots N \tag{8}$$

where x_t is the NINO1.2 data observed in month t, $\omega_j = 2\pi(j-1)/N$, and the A_j and ϕ_j are computed using the Discrete Fourier Transform. The model was fit to the N = 1800 monthly observations of Niño1.2 index from 1856 to 2005. To generate new simulations the phase for each frequency, ϕ_j was randomly drawn from a uniform distribution $\phi_j \sim U[0, 2\pi]$ for $j = 1 \ldots N/2$. A simulated annual series of the NINO1.2 index, consistent with our use for trigger development was then constructed by taking the maximum of the January, February, March, and April monthly Niño1.2 simulated data for each year. These data are then used to construct binary payout sequences v_t (if $x_t > x^*$, $v_t = 1$, else 0), corresponding to each trigger x^* defined earlier.

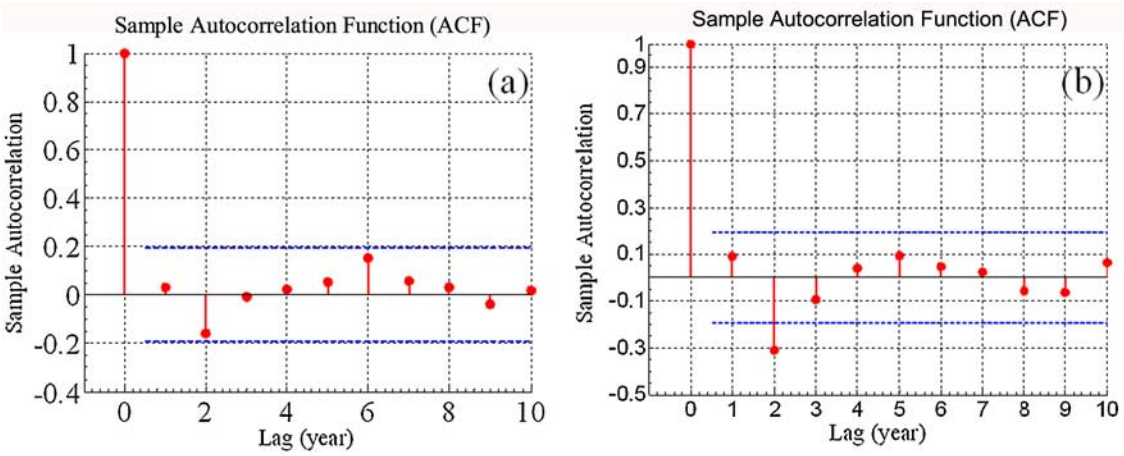

Figure 11. (a) NINO1.2 autocorrelation for the JAFM mean. (b) NINO1.2 lag correlation with NINO3.4.

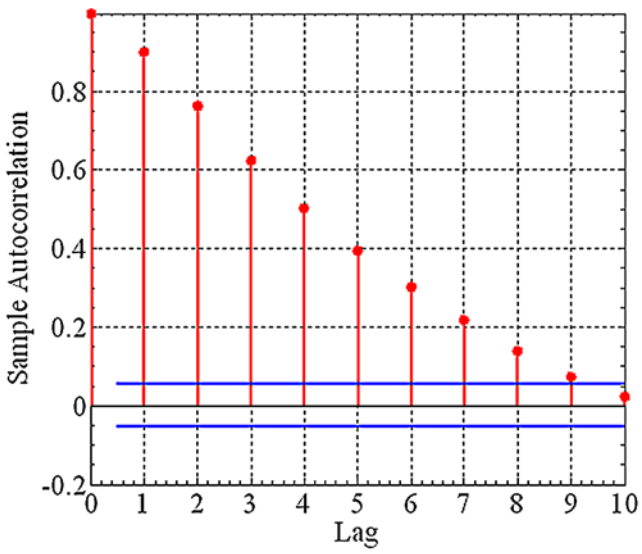

Figure 12. Correlation of the JAFM means NINO1.2 with prior month NINO1.2 values using the 1856–2004 data.

[48] The process was repeated to generate 10,000 sequences, each of 150 years in length. The simulated run length per simulation and the associated uncertainty across the 10,000 sequences corresponding to the two trigger levels are presented in Figure 10. Figure 10 also includes the counts for run lengths as estimated from the historical record and from the raw bootstrap. We note that the probability of run lengths longer than one is larger for the observed sequence and for the spectral bootstrap than for the raw bootstrap, suggesting that there is an enhanced probability of clustering of payouts than would be expected for a time series that has no memory. However, run lengths longer than 2 years are still extremely rare. The observed run length probabilities are near the upper edge of the uncertainty band from the spectral bootstrap, suggesting that a linear time series model (as implied by the spectral bootstrap) will not adequately capture the clustering dynamics of events associated with the two thresholds explored with the NINO1.2 series. Thus, if there was an interest in a formal model to explore event clustering probabilities, then an alternate time series modeling approach would be needed.

[49] In this section, we were able to demonstrate that (1) the NINO1.2-based index results in the correct average exceedance probability in the long run, (2) there is no evidence of monotonic trend in the NINO1.2 series, and (3) there is some evidence of clustering of run lengths for consecutive year payouts at a rate higher than would be expected purely by chance.

3.3. NINO1.2 Index Predictability

[50] A critical question that arises in the design of any risk transfer product is whether the underlying index, and hence the likelihood of payout, can be predicted prior to the purchase of the contract. If this is the case, adverse selection can arise, undermining the actuarial performance of the product.

[51] This question is explored by examining the autocorrelation of the NINO1.2 index and its correlation with the lagged values of the more generally reported NINO 3.4 index. As seen in Figure 11, the NINO1.2 index's correlation with prior values of the NINO1.2 or NINO3.4 index is not significant at the 95% level, suggesting that it cannot be easily predicted in the prior year.

[52] The correlation of the NINO1.2 JAFM data with prior monthly values of the Niño1.2 data is also examined. From Figure 12, it is apparent that the correlation drops approximately geometrically with lag and is about 0.5 at a 4 month lag, suggesting that a linear model would explain only about 25% of the NINO1.2 variance at that lag. By 7 months, the lag correlation has dropped to 0.2 (variance explained = 4%), which is statistically significant, but practically useless for prediction of the future NINO1.2. Thus index insurance sales could be closed about 6 months prior to the flood season, in June of the preceding year, if predictability were a concern.

3.4. Indemnity Analysis

[53] Various structures can be designed for the index insurance payoff. One simple structure for payoff per unit annual premium:

$$I = \frac{\alpha v}{p_{exc}} \tag{9}$$

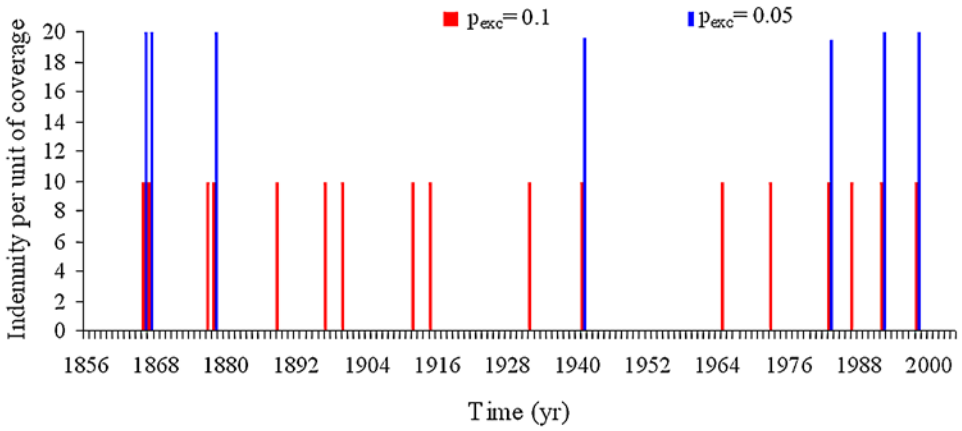

Figure 13. Payoffs per dollar of annual premium over the 1856–2005 period using the NINO1.2 index with the two trigger levels used as an example in this paper. We assume here that $\alpha = 1$.

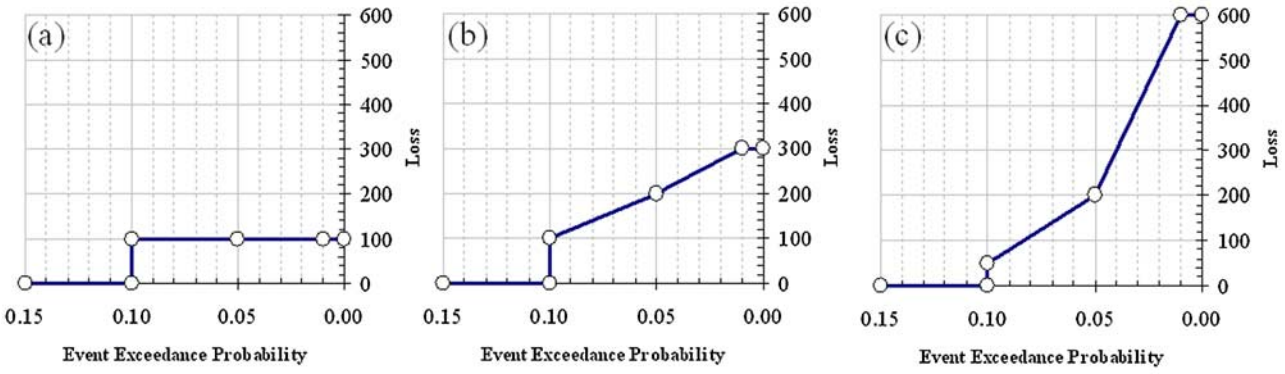

Figure 14. Three hypothetical loss functions for prospective insurance purchasers.

[54] The parameter α reflects the fraction of the payoff residual to the insurer's management fee. If $\alpha = 1$ then there is no management fee and the expected value of the index insurance is 0, since the annual premiums equal the average annual payout in the long run. The resulting indemnity schedule for this payout structure is illustrated in Figure 13, for $\alpha = 1$. An advantage of this payout structure is that it is easy to understand and communicate, and does not presume any knowledge of the purchaser's exposure, risk tolerance or budget.

[55] Let us consider three hypothetical examples of a purchaser's loss function, as illustrated in Figure 14. Insured A, incurs a loss of all her assets (100 units) if a 10 year event occurs; that is, the loss is constant for events more extreme than the 10 year event. In this case, she is best served by buying a policy triggered by a 10 year event with an annual pure premium of 10 units. Insured B, has a loss function that increases linearly with the probability of exceedance associated with the event, starting with the 10 year event up to the 100 year event, at which point he has lost all assets, and incurs a constant loss. B could then choose a mix of index insurance products that could be offered at different risk levels (p_{exc}). For example, he could purchase 10 units of the product offered at $p_{exc} = 0.1$, 5 units of the product offered at $p_{exc} = 0.05$, and 1 unit of the index insurance offered at $p_{exc} = 0.01$. Assuming $\alpha = 1$, this strategy would provide a payoff of 300 units ($100 \times 1 + 20 \times 5 + 10 \times 10$) if a 100 year or larger event occurs ($p_{exc} = 0.01$), of 200 units ($20 \times 5 + 10 \times 10$) if an event with a return period between 20 to 100 years occurs, of 100 units (10×10) if an event with a return period between 10 and 20 years occurs, and 0 if the event is smaller than a 10 year event.

[56] Insured C has a loss function that increases more than linearly with the probability of exceedance of the event, starting with the 10 year event up to the 100 year event at which time all assets are lost. To match this loss exposure pattern, C could choose to buy a different package (5, 8, 4) of the three insurance products ($p_{exc} = 0.1$, 0.05 and 0.01) to approximate this loss function with an appropriate payoff structure (50, 210, 610) for the events of concern.

[57] Thus, given the availability of index insurance products at different risk levels, a consumer could construct an equivalent index insurance product with a graduated payoff structure corresponding to an assessment of exposure at each risk level and cash flow needs in such a contingency. Each potential buyer may have a different loss function, and hence this strategy could be quite flexible. We recommend that index insurance products be offered at trigger levels that correspond to the 10, 20, 50, and 100 return periods. Given available record lengths and the concern with anthropogenic climate change, it may be unwise to offer index insurance products tailored to longer return periods. Catastrophe bonds or other risk management methods may be more suitable in the more extreme cases.

4. Summary and Discussion

[58] The technical objective of the work presented here was to see if a climate index that is recorded by an independent external party could be successfully used as a basis for setting index flood insurance in Peru. Index insurance using weather-related triggers is receiving quite some interest, and there is interest in reliable, independently measured indices that may be well correlated with regional weather or loss triggers. A strategy by which such a product could be developed and its attributes formally assessed has been lacking. Addressing this problem is the contribution of this paper. We demonstrated the following.

[59] 1. Particularly for extreme rainfall events in Peru, the NINO1.2 index appears to be well correlated with a regional flood proxy derived as a superset of multiple regional rainfall records.

[60] 2. A logistic regression-based approach can be used to develop NINO1.2 triggers corresponding to the desired probabilities of exceedance of the regional flood proxy, and that the temporal risk associated with this approach is comparable to that directly using the regional rainfall index.

[61] 3. The use of the NINO1.2-based triggers provides access to a much longer historical record to verify exceedance probabilities and payout frequency attributes including event clustering, and interevent duration statistics.

[62] 4. There is no evidence of a monotonic trend in payoffs over the 150 year NINO1.2 record at the 5% significance level, but one must be cautious with this assertion given the strong evidence of recent anthropogenic climate change (e.g., 3 or 4 events for NINO1.2 that exceed 2 occurred in the last 25 years versus the total of 4 events in the last 100 years).

[63] 5. There is some evidence of payout event clustering beyond what would be expected for the stated exceedance probability for an independent and identically distributed

series – however, we do know that ENSO is a quasi-oscillatory phenomena so this is not unexpected.

[64] 6. The likelihood that the NINO1.2 index can be predicted using simple techniques with lead times of 6 months or more is low, suggesting that appropriate sales strategies could be developed to account for this potential.

[65] 7. All index insurance products have some residual basis risk since the payout is only related to the outcome and is not based on an actual damage. This is not addressed in this paper.

[66] Insurance companies may use such an index with a variety of indemnity payoff structures. Where such systems are transparent and fair with a clear application strategy they will be effective in serving and attracting customers. The detailed economic analysis of insurance product design and its effectiveness was not pursued in this paper, but will be covered in a subsequent paper. We restricted our attention to the investigation of the attributes of the climatic time series that would help design and evaluate such a product. To our knowledge no comparable work looking at the statistical attributes of a climate proxy as an indicator exists. The work presented here could be used as a template for the investigation of other climate indices for the same purpose in other locations.

[67] Finally, while we motivated this paper with the need to develop a flood index insurance product for Peru using an external climate index, it may be obvious at this stage that a global offering of an index insurance product tied to an ENSO index may be feasible as a risk management strategy. A fundamental tenet of insurance is that if we can pool a large number of uncorrelated or negatively correlated risks, then we end up with a more robust risk management product for the insurer, since the variance (as measured by the coefficient of variation) in payouts is decreased, and also the total size of the cash flow is larger enabling resilience to large individual payouts. We know [*Indeje et al.*, 2000; *Ogallo*, 1993; *Ogallo et al.*, 2000] that ENSO has far-reaching socioeconomic impacts through its correlation with flood and drought in many parts of the world. The index insurance product could be developed to address both the flood and the drought side of the risk, and offering it globally would allow both the countries at risk and potential donor countries to contribute to a common pool for financial risk management. Since the correlation of floods and droughts and the corresponding losses with the ENSO index will vary by country (location), the product would be marketed by triggers derived directly from the exceedance probability distribution of the ENSO index, and an analyst in a particular location who wishes to create a local insurance portfolio would have to assess the exceedance probability of a certain loss in the country corresponding to an ENSO event (x*) at a designated probability of exceedance p_{exc}. Where historical climate and loss data are available, this could be accomplished using appropriate statistical models that link the ENSO index to the local time series. Where local data are not available, but there is evidence that ENSO events lead to adverse outcomes, the ENSO index could be purchased directly at the advertised exceedance probabilities, since in a field of imperfect information as to losses and their incidence rate it may be the best available proxy.

[68] **Acknowledgments.** This research was partially supported using USAID funding under a project that was conducted between COPEME of Peru and GlobalAgRisk, Inc., of Lexington, Kentucky. We thank Arthur Small III and two anonymous referees for their comments that led to an improvement of our original manuscript.

References

Bardsley, P., A. Abey, and S. Davenport (1984), The economics of insuring crops against drought, *Aust. J. Agric. Econ.*, *28*, 1–14.

Changnon, S. A., et al. (2001), Losses caused by weather and climate extremes: A national index for the United States, *Phys. Geogr.*, *22*, 1–27.

Chichilnisky, G., and G. Heal (1998), Managing unknown risks, *J. Portfolio Manage.*, *24*, 85–91.

Cleveland, W. S. (1979), Robust locally weighted regression and smoothing scatterplots, *J. Am. Stat. Assoc.*, *74*, *368*, 829–836.

Duncan, J., and R. J. Myers (2000), Crop insurance under catastrophic risk, *Am. J. Agric. Econ.*, *82*, 842–855.

Gilks, W. R., et al. (1995), Adaptive rejection metropolis sampling within Gibbs sampling, *Appl. Stat. J. R. Stat. Soc., Ser. C*, *44*, 455–472.

Glantz, M. H. (Ed.) (2001), *Once Burned, Twice Shy? Lessons Learned from the 1997–98 El Niño*, U.N. Univ., Tokyo.

Hess, U., J. Skees, A. Stoppa, B. Barnett, and J. Nash (2005), Managing agricultural production risk: Innovations in developing countries, *Rep. 32727-GLB*, Agric. and Rural Dev. Dep., World Bank, Washington, D. C.

Indeje, M., F. H. M. Semazzi, and L. J. Ogallo (2000), ENSO signals in East African rainfall seasons, *Int. J. Climatol.*, *20*, 19–46.

Luo, H., J. R. Skees, and M. A. Marchant (1994), Weather information and the potential for intertemporal adverse selection in crop insurance, *Rev. Agric. Econ.*, *16*, 441–451.

Mann, M. E., and J. Park (1994), Global-scale modes of surface temperature variability on interannual to century timescales, *J. Geophys. Res.*, *99*, 25,819–25,834.

Mann, M. E., R. S. Bradley, and M. K. Hughes (1998a), Global-scale temperature patterns and climate forcing over the past six centuries, *Nature*, *392*, 779–787. (Correction, *Nature*, *430*, 105, 2004.)

Mann, M. E., R. S. Bradley, and M. K. Hughes (1998b), Global temperature patterns, *Science*, *280*, 2029–2030.

Martin, S. W., B. J. Barnett, and K. H. Coble (2001), Developing and pricing precipitation insurance, *J. Agric. Resour. Econ.*, *26*, 261–274.

Miranda, M. J. (1991), Area-yield crop insurance reconsidered, *Am. J. Agric. Econ.*, *73*, 233–242.

Miranda, M. J., and J. W. Glauber (1997), Systemic risk, reinsurance, and the failure of crop insurance markets, *Am. J. Agric. Econ.*, *79*, 206–215.

Ogallo, L. A. (1993), Dynamics of the East-African climate, *Proc. Ind. Acad. Sci. Earth Planet. Sci.*, *102*, 203–217.

Ogallo, L. A., M. S. Boulahya, and T. Keane (2000), Applications of seasonal to interannual climate prediction in agricultural planning and operations, *Agric. For. Meteorol.*, *103*, 159–166.

Podesta, G., D. Letson, C. Messina, F. Royce, R. A. Ferreyra, J. Jones, J. Hansen, I. Liovet, M. Grondona, and J. J. O'Brien (2002), Use of ENSO-related climate information in agricultural decision making in Argentina: A pilot experience, *Agric. Syst.*, *74*, 371–392.

Rosenzweig, C., F. N. Tubiello, R. Goldberg, E. Mills, and J. Bloomfield (2002), Increased crop damage in the US from excess precipitation under climate change, *Global Environ. Change Human Policy Dimensions*, *12*, 197–202.

Ropelewski, C. F., and M. S. Halpert (1987), Global and regional scale precipitation patterns associated with the El Niño/Southern Oscillation, *Mon. Weather Rev.*, *115*, 1606–1626.

Ropelewski, C. F., and M. S. Halpert (1989), Precipitation patterns associated with the high index phase of the Southern Oscillation, *J. Clim.*, *2*, 268–284.

Salas, J. D. (1992), Analysis and modeling of hydrologic time series, in *Handbook of Hydrology*, edited by D. R. Maidment, chap. 19, pp. 19.1–12.72, McGraw-Hill, New York.

Skees, J. R., and B. J. Barnett (1999), Conceptual and practical considerations for sharing catastrophic/systemic risks, *Rev. Agric. Econ.*, *21*, 424–441.

Skees, J. R., and M. R. Reed (1986), Rate making for farm-level crop insurance—Implications for adverse selection, *Am. J. Agric. Econ.*, *68*, 653–659.

Skees, J. R., J. R. Black, and B. J. Barnett (1997), Designing and rating an area yield crop insurance contract, *Am. J. Agric. Econ.*, *79*, 430–438.

Skees, J. R., B. J. Barnett, and J. Hartell (2005), Innovations in government response for catastrophic risk sharing for agriculture in developing countries, report, Commod. Risk Manage. Group, Agric. And Rural Dev. Dep, World Bank, Washington, D. C.

Spiegelhalter, D. J. (1998), Bayesian graphical modelling: A case-study in monitoring health outcomes, *J. R. Stat. Soc., Ser. B*, *47*, 115–133.

Spiegelhalter, D. J., N. G. Best, B. R. Carlin, and A. van der Linde (2002), Bayesian measures of model complexity and fit, *J. R. Stat. Soc., Ser. B*, *64*, 583–616.

Stigter, C. J., D. W. Zheng, L. O. Z. Onyewotu, and X. R. Mei (2005), Using traditional methods and indigenous technologies for coping with climate variability, *Clim. Change*, *70*, 255–271.

Tapley, T., and P. Waylen (1990), Spatial variability of annual precipitation and ENSO events in western Peru, *Hydrol. Sci.*, *35*(4), 429–446.

Wall, E., and B. Smit (2005), Climate change adaptation in light of sustainable agriculture, *J. Sustainable Agric.*, *27*, 113–123.

Woolhiser, D. A., T. O. Keefer, and K. T. Redmond (1993), Southern Oscillation effects on daily precipitation in the southwestern United States, *Water Resour. Res.*, *29*(4), 1287–1296.

Xie, P. P., and P. A. Arkin (1996), Analyses of global monthly precipitation using gauge observations, satellite estimates, and numerical model predictions, *J. Clim.*, *9*, 840–858.

Xie, P. P., and P. A. Arkin (1997), Global precipitation: A 17-year monthly analysis based on gauge observations, satellite estimates, and numerical model outputs, *Bull. Am. Meteorol. Soc.*, *78*, 2539–2558.

Xie, P., B. Rudolf, U. Schneider, and P. A. Arkin (1996), Gauge-based monthly analysis of global land precipitation from 1971 to 1994, *J. Geophys. Res.*, *101*, 19,023–19,034.

A. F. Khalil, H.-H. Kwon, and U. Lall, Department of Earth and Environmental Engineering, Columbia University, 918 S. W. Mudd, mail code 4711, New York, NY 10027, USA. (hk2273@columbia.edu)

M. J. Miranda, Department of Agricultural, Environmental, and Development Economics, Ohio State University, 2120 Fyffe Road, Columbus, OH 43210-1067, USA.

J. Skees, Department of Agricultural Economics, University of Kentucky, 310 Charles E. Barnhart Building, Lexington, KY 40546-0276, USA.